IN-SITU LAYER-WISE GEOMETRY EXTRACTION OF THIN-WALL 316L STRUCTURES FABRICATED BY LASER POWDER BED FUSION

Digambar Killedar[a], Mumin Adhami[a], Can Sun[a], Mateo E. Garcia-Sandoval[a], Austin R.J. Downey[a, b], Yanzhou Fu[c], Lang Yuan[a], and Yash Parikh[d]

[a] Department of Mechanical Engineering, University of South Carolina, Columbia, SC, USA

[b] Department of Civil and Environmental Engineering, University of South Carolina, Columbia, SC, USA

[c] Department of Ocean and Mechanical Engineering, Florida Atlantic University, Boca Raton, FL, USA

[d] EOS of North America, Inc., Pflugerville, TX, USA

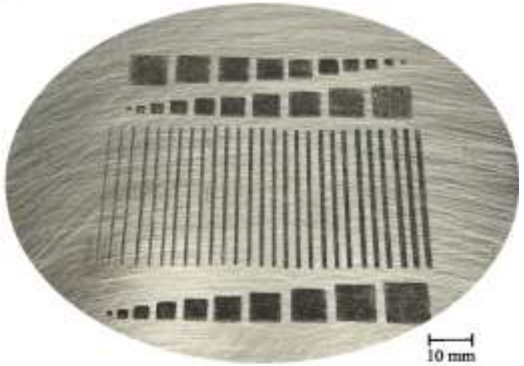

UNIVERSITY OF
South Carolina
Molinaroli College of
Engineering and Computing

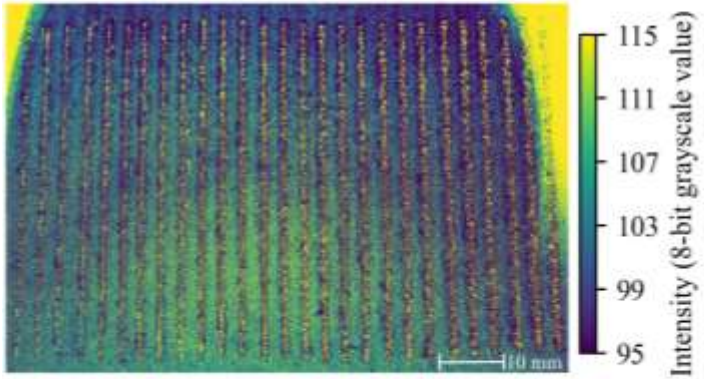

Introduction

Challenge

- LPBF is used for complicated manufacturing.
- Thin-wall parts are highly sensitive to thermal effect.
- Small defects can significantly impact structural integrity.
- Thermal gradients induce residual stress and distortion.
- Layer-by-layer deposition leads to error accumulation.

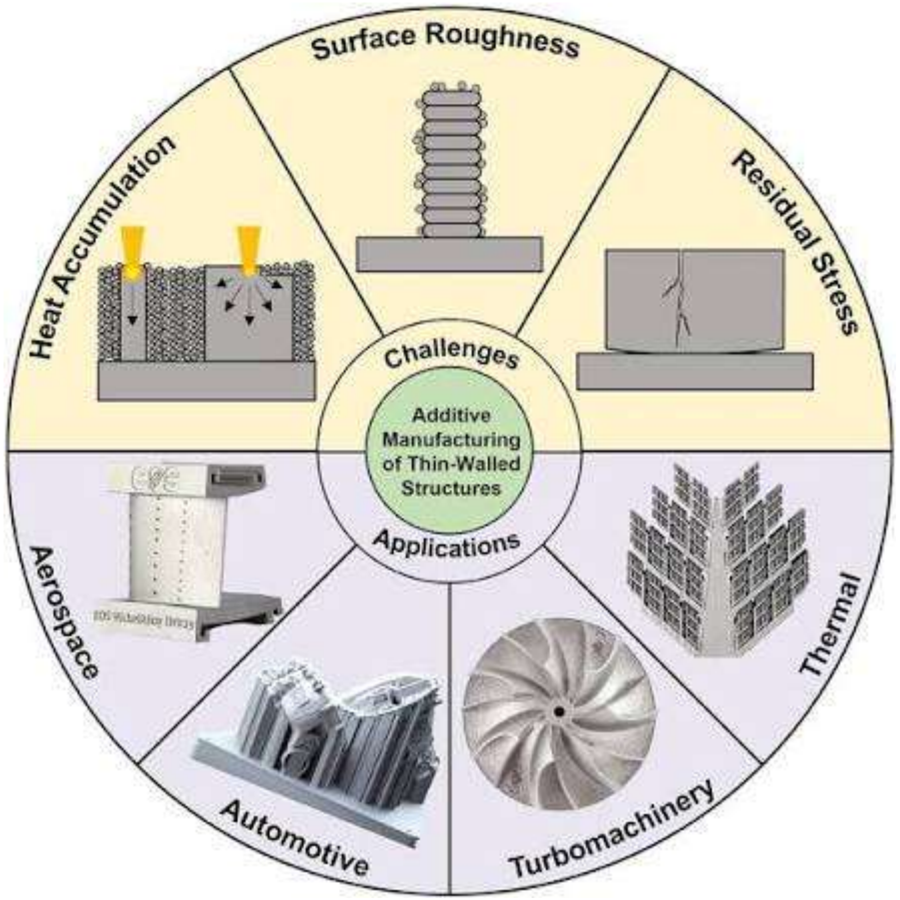

P. Viveganathan, S. Gao, W. Ji, H. Fan, C. Han, K. Zhou, *Recent Progress on 3D Printing of Lightweight Metal Thin-Walled Structures*. *Adv. Mater.* 2024, 36, 2402130. https://doi.org/10.1002/adma.202402130

Goal: Parts Ready for Use After Printing

- Enable parts to be ready for use immediately after printing
- Eliminate reliance on post-process testing
- Detect defects and assess impact as they occur
- Move toward in-process validation and certification

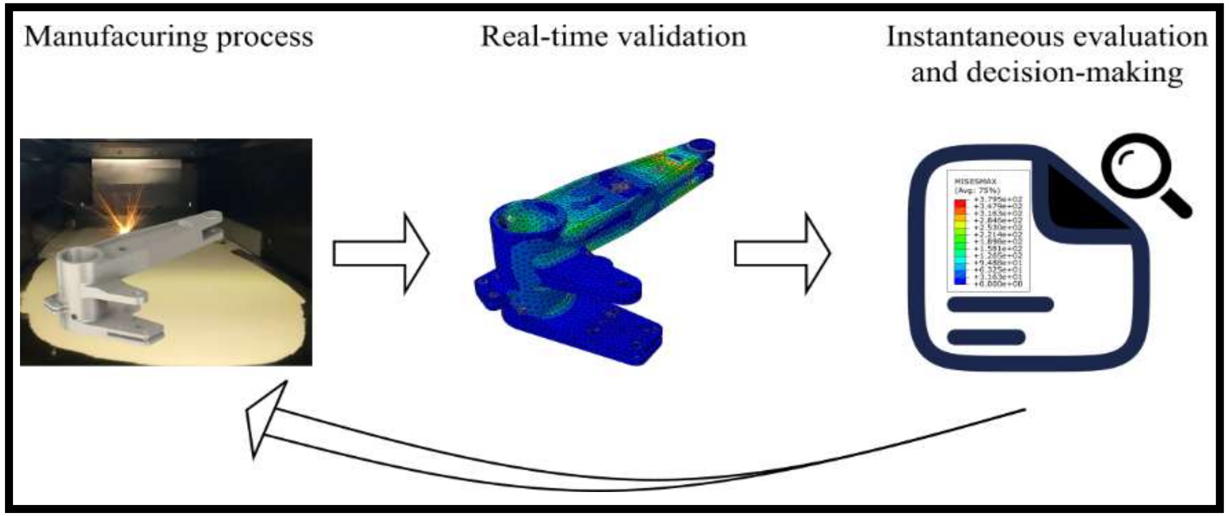

Overarching goal

Goal

- Enable parts to be ready for use immediately after printing.
- Eliminate reliance on postprocess testing.
- Detect defects and assess impact as they occur.
- Move toward in-process validation and certification.

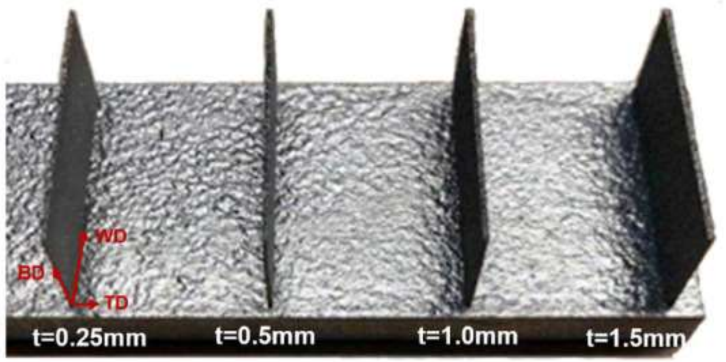

Yiming Sun, Hongyun Zhao, Rongrong Huang, Linchuan Liu, et.al., Journal of Materials Research and Technology, Volume 27, 2023, Pages 703-717, https://doi.org/10.1016/j.jmrt.2023.10.025.

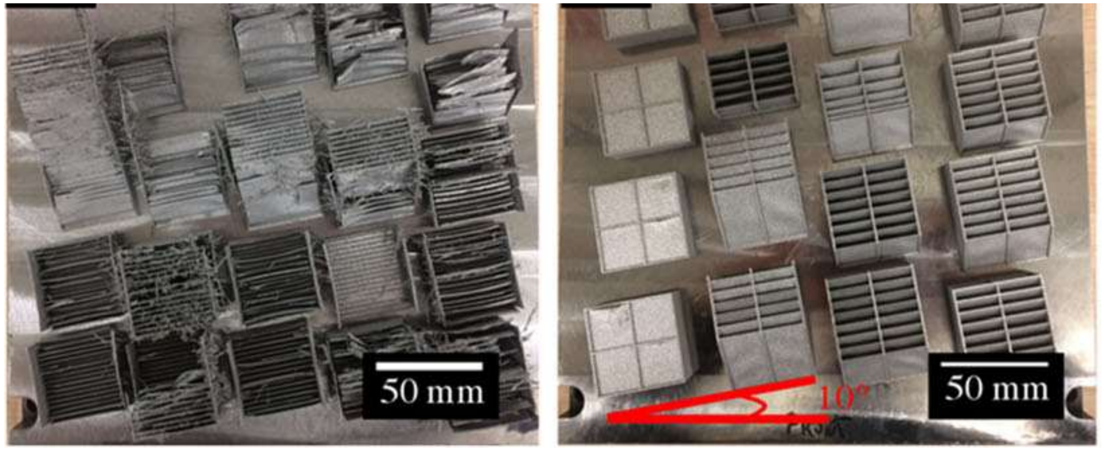

Wu, Ziheng & Narra, Sneha & Rollett, Anthony. (2020). Exploring the fabrication limits of thin-wall structures in a laser powder bed fusion process. The International Journal of Advanced Manufacturing Technology. 110.10.1007/s00170-020-05827-4

Why thin-wall structures matter in AM

- Thin walls appear in lightweight load-bearing parts, heat sinks, lattice-supported architectures, and biomedical devices.
- Issues of wall distortion, thickness variation, and lateral movement due to repeated laser heating, rapid cooling, thermal gradients, and re-coater interaction.
- Small cross-section and low bending stiffness amplify dimensional variation.
- Final wall geometry affects thickness, shape, and structural integrity.

P. Viveganathan, S. Gao, W. Ji, H. Fan, C. Han, K. Zhou, *Recent Progress on 3D Printing of Lightweight Metal Thin-Walled Structures*. *Adv. Mater.* 2024, 36, 2402130. https://doi.org/10.1002/adma.202402130

Contributions of the current study

- Direct extraction of wall lateral geometric shift/ deviations and thickness as quantitative layer-wise observables.
- A practical vision-based methodology for reconstructing thin-wall boundaries from in-situ optical data.
- An experimental analysis showing how these measurements reveal thickness-dependent geometric trends in LPBF-fabricated 316L thin walls.
- This framework provides a foundation for future physics-based monitoring and digital-twin-enabled process control in metal additive manufacturing.

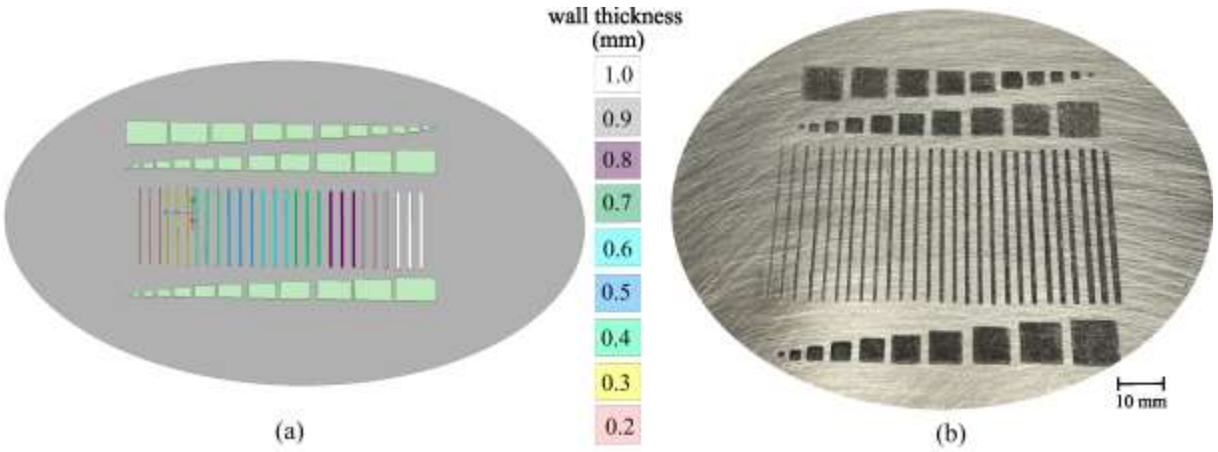

Fig : (a) CAD of printed wall , (b) actual 3D printed wall

Experiment system

Can fixed layer-wise optical images be transformed into quantitative, physically interpretable geometric observables for LPBF thin-wall structures?

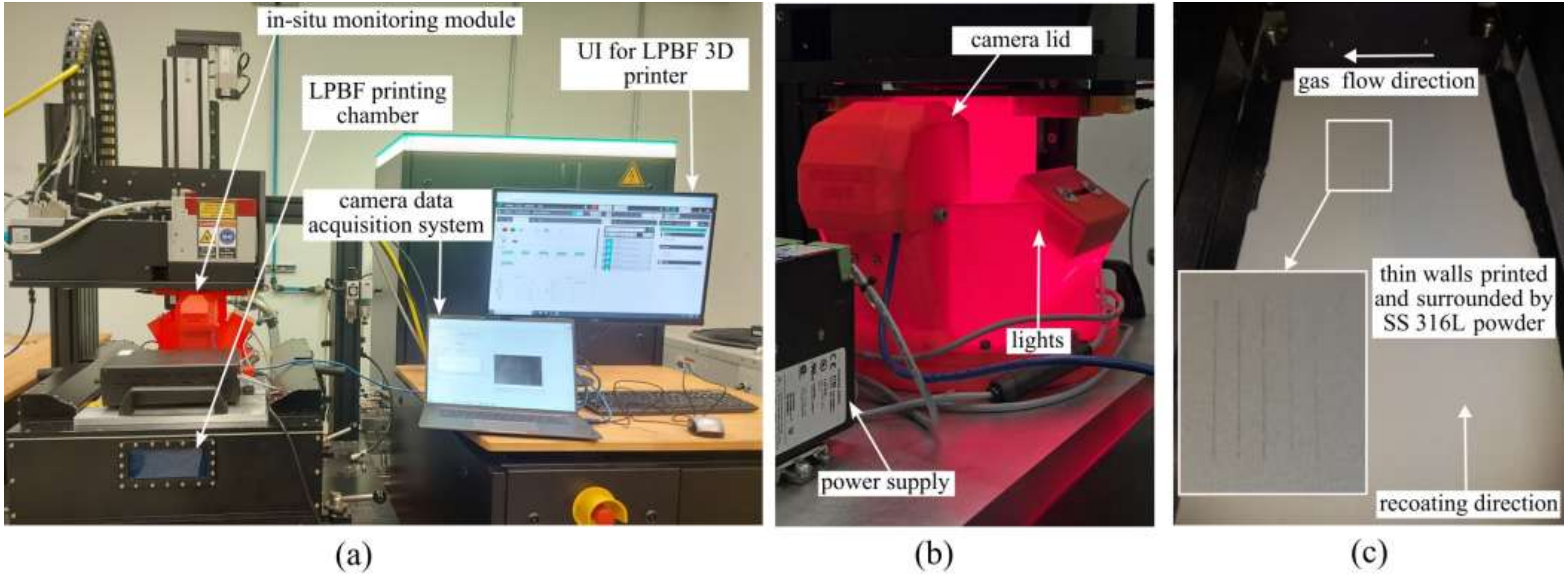

Fig. Experimental setup for LPBF thin-wall fabrication and in-situ monitoring, showing: (a) 3D printer along with data acquisition system; (b) side view of in-situ monitoring module and; (c) SS 316L powder spread on the print bed.

Experiment system

- The dedicated enclosure is developed for Aconity MIDI metal 3D printer.
- Gas-atomized SS316L powder (Carpenter Technology, Germany) used for 3D printing
- Camera used : FLIR Blackfly USB 3.0 camera (BFS-200S6M-C Teledyne FLIR) equipped with a 20 MP monochrome, 1-inch sensor (Sony IMX183)
- Lens used : Edmund Optics fixed lens (86573, 35 mm/F1.8, C-Series)
- Advanced Illumination 2 × 3 LED spotlights (AL143-625IC) along with Midwest Optical Systems bandpass filter (BP635-37).

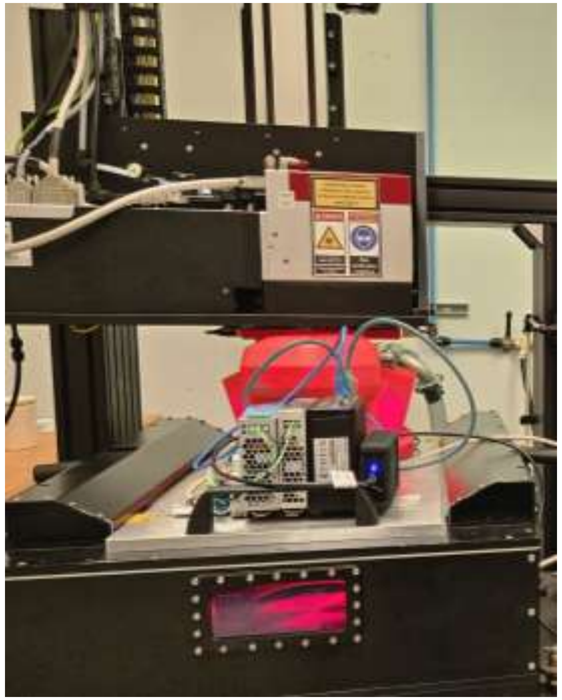

Fig. Enclosure for in-situ monitoring

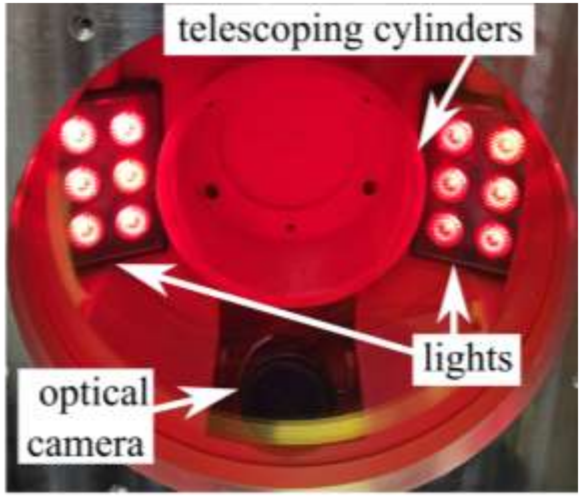

Fig. Camera and LED arrangements

Digital Twin: Concept and Framework

Digital Twin: Concept and Vision

- Virtual representation of a physical counterpart
- Updated using data from the physical counterpart
- Enables prediction, monitoring, and decision-making
- Information flows between physical and virtual systems
- Supports decisions on system performance

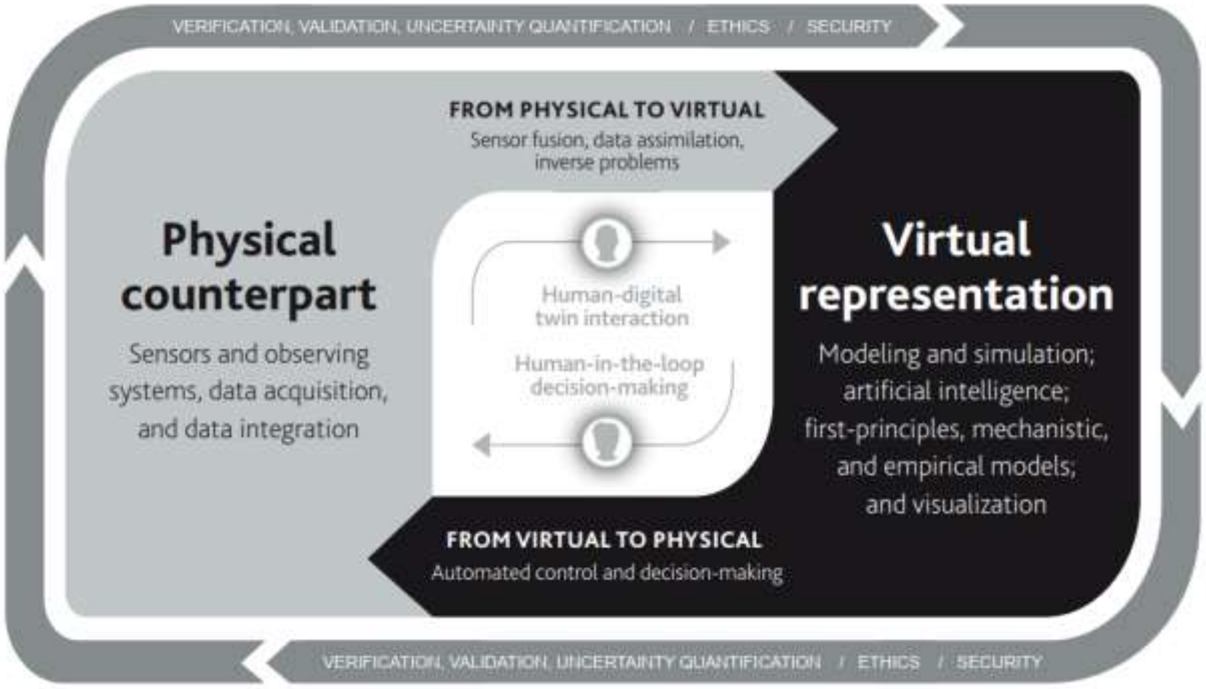

National Academies of Sciences, Engineering, and Medicine. 2024. Foundational Research Gaps and Future Directions for Digital Twins. Washington, DC: The National Academies Press.

Interacting with the Digital Twin

- Enables a query–response interaction
- Physical counterpart provides measurements
- Queries probe the virtual representation
- Virtual representation returns predictions
- Responses guide actions on the physical counterpart

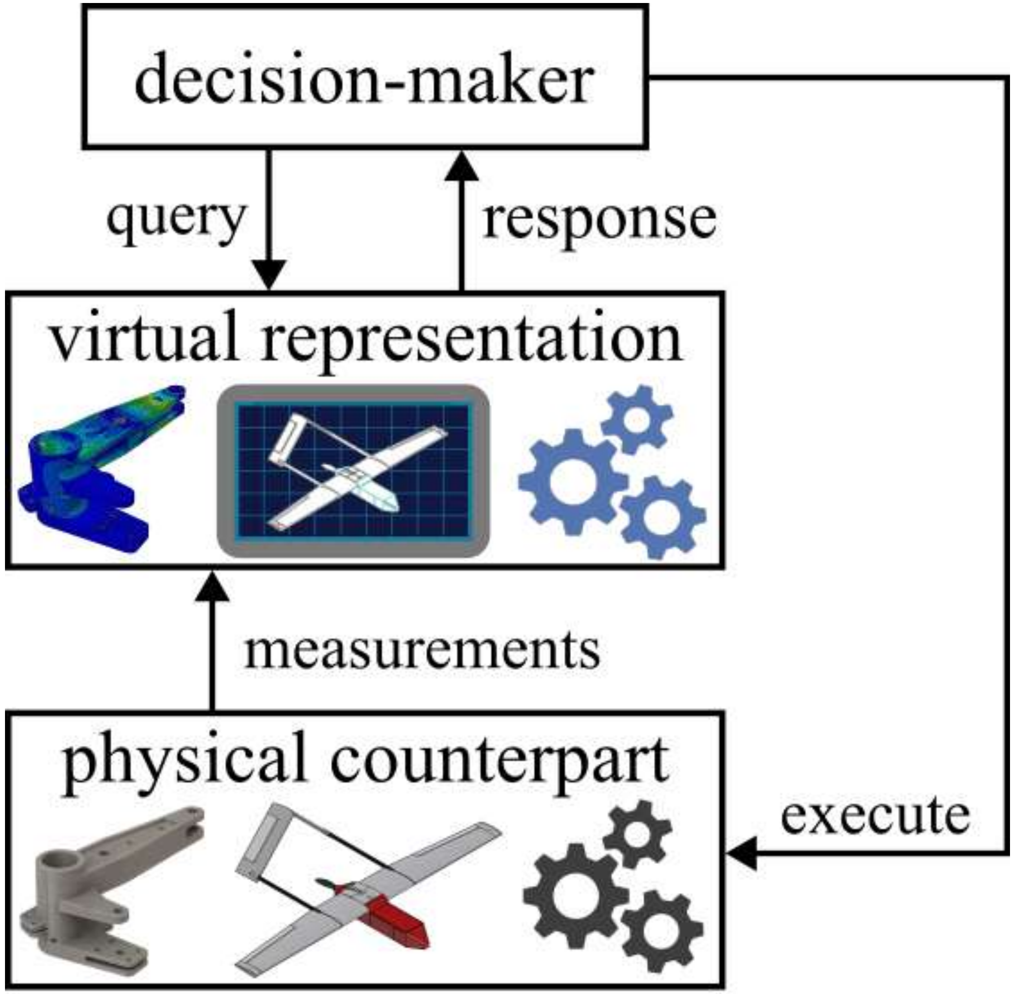

Kerry Sado, Jarrett Peskar, Austin R.J. Downey, Herbert L. Ginn, Roger Dougal, and Kristen Booth. Query-and-response digital twin framework using a multi-domain, multifunction image folio. *IEEE Transactions on Transportation Electrification*, pages 1-1, 2024. doi:10.1109/tte.2024.3425276

Methodology and Approach

Initial layers : LPBF build + in-situ optical imaging

- Aconity MIDI LPBF system with SS316L powder.
- Nominal wall thicknesses from 0.2 mm to 1.0 mm.
- Fixed optical camera records grayscale surface images after successive layers at defined intervals using LabView VI
- Images properties are adjusted in-situ and saved.

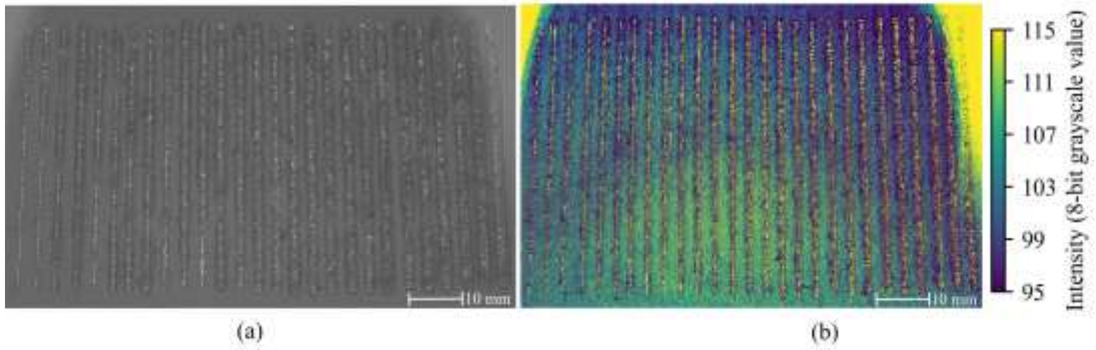

Fig. Representative in-situ optical images of the LPBF build surface, showing: (a) a monochrome, uncropped raw image of the printed walls on the build plate and; (b) a viridis colormap representation of the printed walls.

Element	Iron	Ni	Cr	O	Si	S	P	N	C	Mo	Mg	Cu
Weight percent (%)	Bal.	12.7	17.7	0.03	0.62	0.01	0.01	0.10	0.02	2.36	0.65	0.02

Fig. Nominal chemical composition of stainless steel 316L, expressed in weight percent (%).

Computer vision workflow for geometry extraction

Major steps of CV pipeline,

1. Read LPBF printed wall image
2. Gaussian convolution using 5X5 kernel on every pixel of an image
3. Intensity averaging to get smooth LPBF printed wall contour.
4. Spot the difference in intensity and define printed wall.
5. Happens over every layer at every pixel of the image

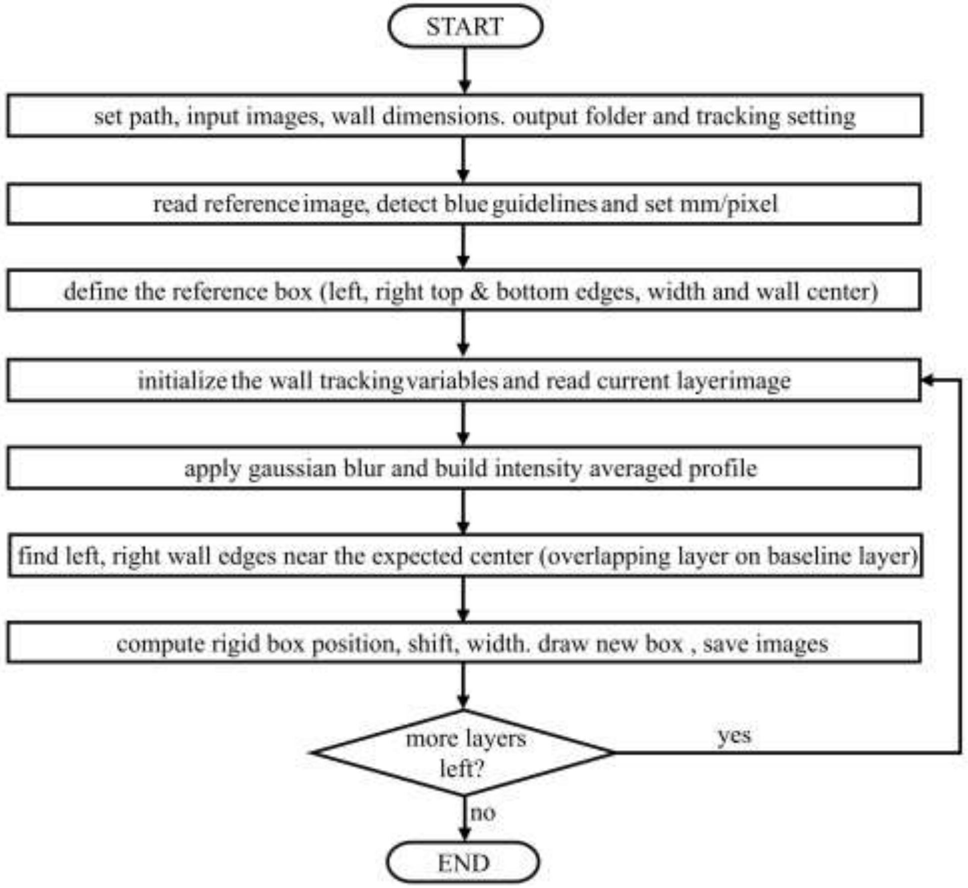

Image processing CV pipeline details

<u>Baseline geometry details</u>,

Wall width, W
Wall length, L = 100 mm
Number of layers, n = 7
Layer thickness, t

H = nt = 7 X 0.03 = 0.21 mm

<u>Reference-box calibration,</u>

Blue-line spacing: Wpx (38 pixels)

Vertical blue-line span: Lpx (1364 pixels)

Sx and Sy are horizontal and vertical image scales respectively based on image pixel and dimensions

$$s_x = \frac{W}{W_{\text{px}}} \qquad s_y = \frac{L}{L_{\text{px}}}$$

Fig. The marked known geometry

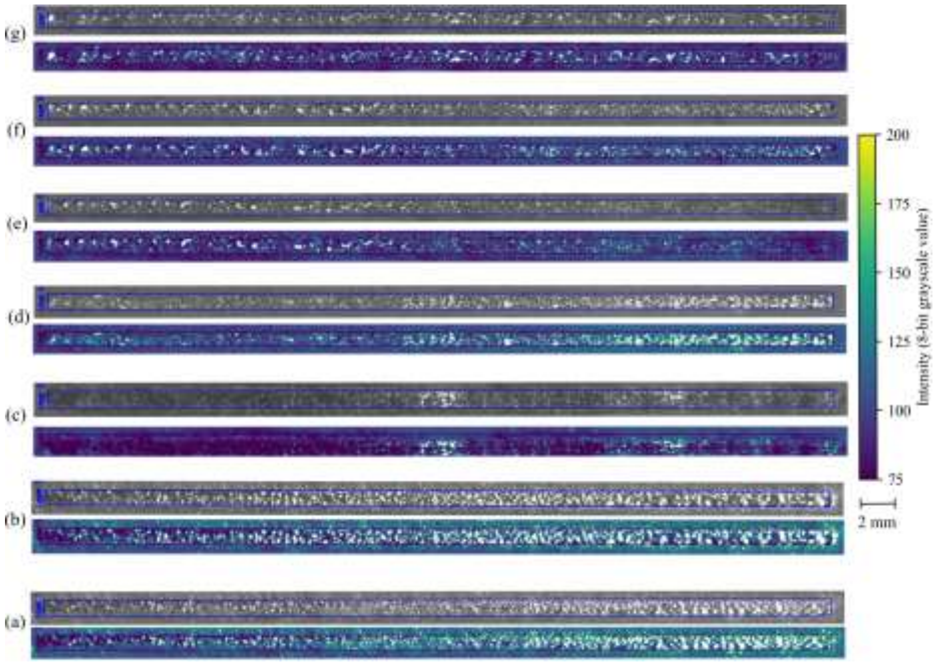

Fig : Wall and edge detection for layer 1 to layer 7 for thin wall design reported in gray scale and viridis for each layer, showing: (a) layer 1; (b) layer 2; (c) layer 3; (d) layer 4; (e) layer 5; (f) layer 6 and; (g) layer 7.

Gaussian blur: suppressing speckle before locating the box

2D Gaussian kernel (filter),

$$G_\sigma(u,v) = \frac{1}{2\pi\sigma^2}\exp\left[-\frac{u^2+v^2}{2\sigma^2}\right]$$

Filtered image (Gaussian convolution),

$$I_\sigma(x,y) = (G_\sigma * I)(x,y)$$
$$= \sum_u \sum_v G_\sigma(u,v)\, I(x-u, y-v)$$

What it does to image,

- Suppress isolated bright particles, pixel noise, and local reflectance spikes before determining the box location.
- Helps in stabilizing the wall box center search.
- Wall width is not measured here yet.

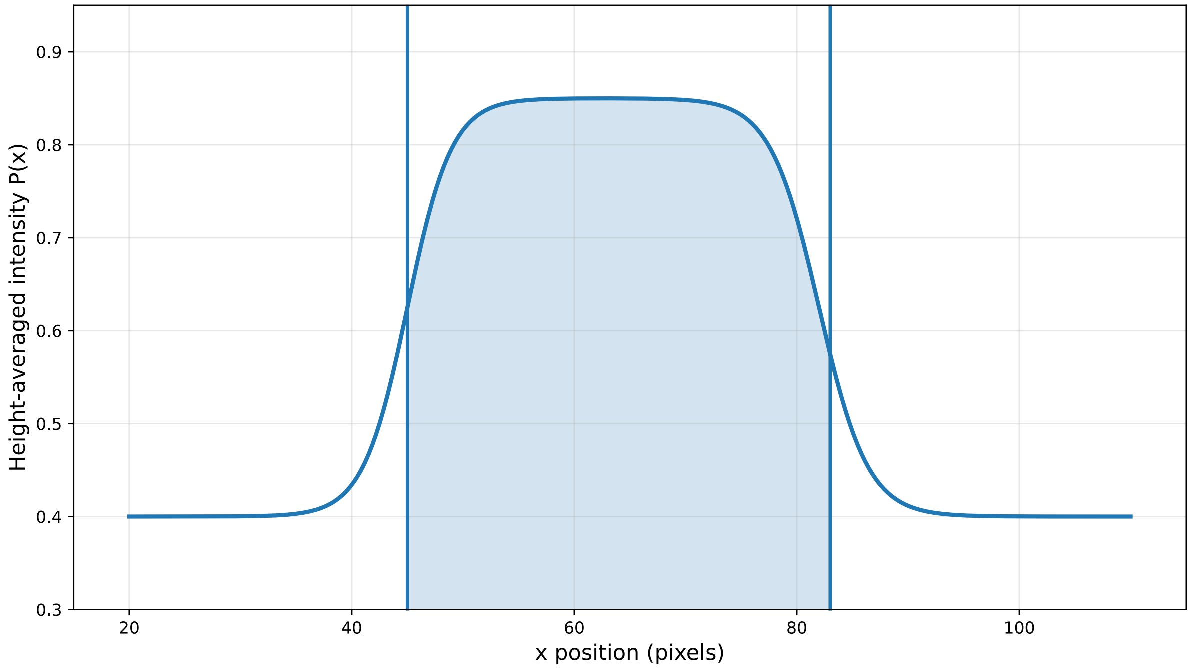

Fig. Gaussian-smoother profile used to place box around printed wall

Height-averaged intensity profile

<u>Profile definition,</u>

$$P_i(x) = \frac{1}{N_y} \sum_{y=y_T}^{y_B} I_{\sigma,i}(x,y)$$

- After smoothing, the two-dimensional image is reduced to a one-dimensional horizontal profile.
- The LPBF wall has random bright and dark speckles along its length. Averaging along y keeps the consistent wall location while reducing local surface-texture noise.
- For every horizontal position x, the algorithm averages all pixel intensities along the 100 mm wall length.

The number of rows is,

$$y_T \leq y \leq y_B \quad \leftrightarrow \quad L = 100\,\text{mm}$$

The resulting profile $P_i(x)$ is then used to select the best box center c_i.

Box centerline and lateral-shift calculation

Candidate box at center c,

Right edge identification, $x_L(c) = c - \frac{W_{\text{px}}}{2}$

Left edge identification, $x_R(c) = c + \frac{W_{\text{px}}}{2}$

Average intensity, $\mu_{\text{inside}}(c) = \frac{1}{W_{\text{px}}} \sum_{x=x_L(c)}^{x_R(c)} P_i(x)$

Average intensity, $\mu_{\text{bg}}(c) = \frac{1}{2}[\mu_{\text{left}}(c) + \mu_{\text{right}}(c)]$

Developed Box score, $S_i(c) = \mu_{\text{inside}}(c) - \mu_{\text{bg}}(c)$

Best center and drift,

$$c_i^* = \arg\max_c S_i(c)$$

Search is restricted near the expected wall position so that neighboring reflections are not selected,

$$c \in [c_0 - d,\ c_0 + d]$$

$$\Delta x_i = c_i^* - c_1^*$$

Centre-line drift of the layer, $\Delta X_i = s_x \Delta x_i$

3D image reconstruction

Layer slice definition,

$$B_i = \{(x, y, z):$$

$$x \in [\Delta X_i - \frac{W}{2},\ \Delta X_i + \frac{W}{2}],$$

$$y \in [-\frac{L}{2},\ \frac{L}{2}],$$

$$z \in [(i-1)t,\ it]\}$$

- Each layer is stacked over another,
- Figure shows 3D reconstruction of printed seven layers

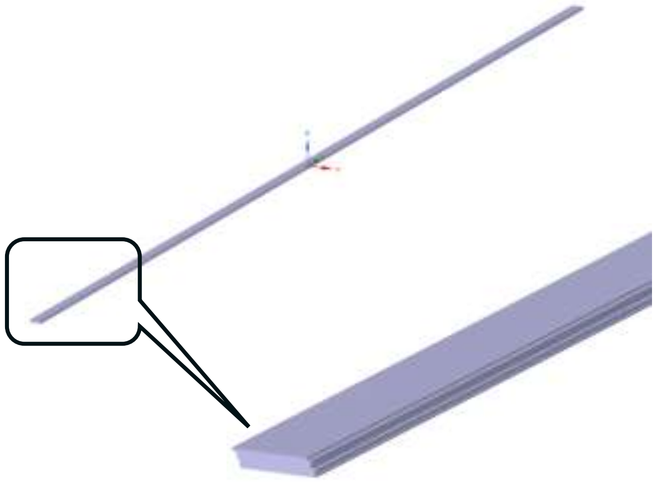

Fig : Full 3D reconstruction of wall

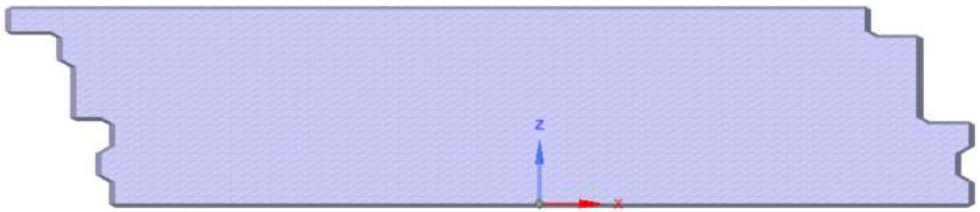

Fig : Cross sectional view

Results and discussion

Thickness measurements

- Measured thickness increases nearly linearly with designed thickness.
- Thicker walls show greater variation from the designed geometry.
- We attribute this to thickness-dependent cooling and solidification, which alter the final wall contour.

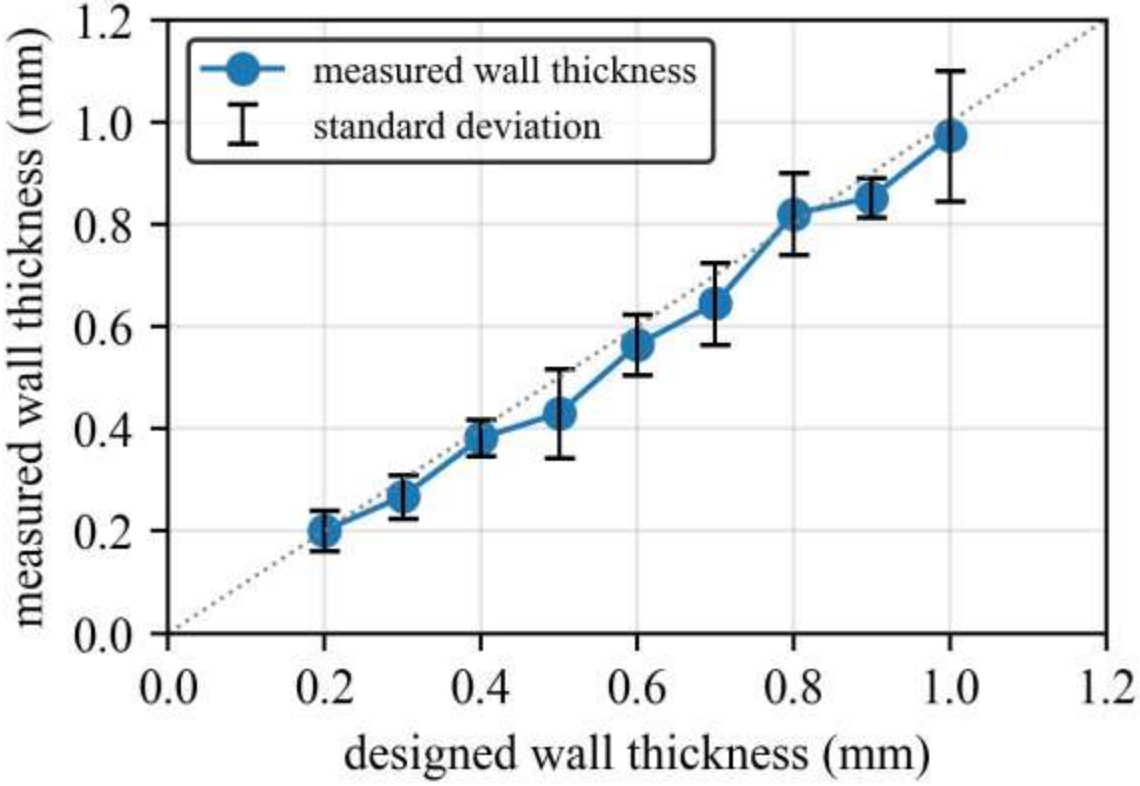

Drift measurements

- Wall drift remains near zero from 0.2 to 0.7 mm.
- Drift and variability increase sharply for the thickest walls.
- We attribute this to larger volumes of molten metal cooling and contracting, making thicker walls more likely to shift.

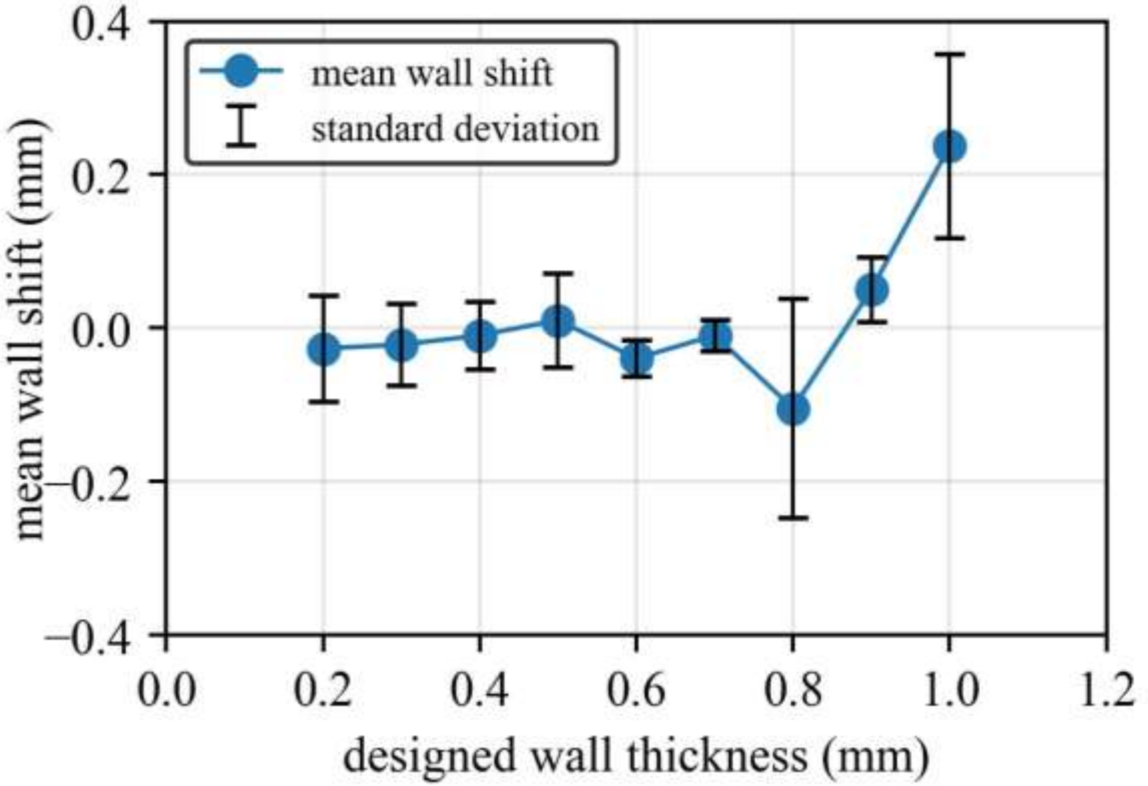

Acknowledgement

This research was supported by the United States' National Science Foundation (NSF), USA, Grants Nos.CCF-2503055, and CPS-2237696. This work is also partially supported by the National Institute of Standards & Technology, United States, under grant number 70NANB23H030, as well as the South Carolina Space Grant Consortium under grants 21-117-RID RGP-SC-009, 25-073-REAP-SC-001, and 25-073-BTC-SC-001. Additional support is provided by the United States' National Science Foundation (NSF) through the NSF ASEE Fellowship. Any opinions, findings, conclusions, or recommendations expressed in this material are those of the authors and do not necessarily reflect the views of the National Science Foundation, the South Carolina Space Grant Consortium, or the National Institute of Standards & Technology.

Discussion

Paper-2026-Geometry-Thin-wall-Laser-Powder-Bed-Fusion

https://github.com/ARTS-Laboratory/Paper-2026-Geometry-Thin-wall-Laser-Powder-Bed-Fusion

Author Information
Name: Austin R. J. Downey
Email: austindowney@sc.edu
GitHub: github.com/austindowney

Molinaroli College of Engineering and Computing
UNIVERSITY OF SOUTH CAROLINA

Physical interpretation: why geometry evolves

Thermal gradients	Narrow walls experience steep thermal gradients and repeated reheating, causing cumulative local distortion.
Heat dissipation limits	Major heat dissipation happens only in one direction due to plain strain condition
Re-coater interaction	Local protrusions can interact with re-coater forces and produce apparent lateral movement or deformation